Heliyon 8 (2022) e11721

Contents lists available at ScienceDirect

Heliyon

journal homepage: www.cell.com/heliyon

Research article

Design of pattern-reconfigurable circularly polarized unidirectional antenna based on quasi-radiator for ISM applications

Philip Arthur, Mubarak Sani Ellis *, Abdul-Rahman Ahmed, Jerry John Kponyo

Department of Telecommunication Engineering, Kwame Nkrumah University of Science and Technology, Kumasi-Ghana

ARTICLE INFO

Keywords:
Pattern-reconfigurable
PIN diode
Circular polarization
Unidirectional radiation

ABSTRACT

A pattern-reconfigurable circularly polarized antenna for 2.45 GHz industrial, scientific, and medical (ISM) band applications is designed in this work. The proposed antenna consists of a slotted-stepped monopole connected to a rectangular ground plane via a shorting side-stub. This converts the omnidirectional radiation pattern of the antenna into stable unidirectional radiation. To dynamically steer the realized pattern, two switchable RF PIN diodes are jointly incorporated into the side-stubs to achieve symmetrical radiations in specific operating modes. In this way, the radiation patterns can be simultaneously tuned in the $\pm y$ directions by the simple switching of the PIN diodes ON and OFF. The fabricated prototype achieves an S_{11} smaller than -10dB within the 3dB axial ratio (AR) bandwidth with stable far-field patterns. The antenna maintains a low-profile and compact size of $0.055\lambda_0^2$ which makes it suitable for body-centric wireless communication (BWC) and personal wireless area networks.

1. Introduction

Many applications in modern wireless communications have driven the need for antennas to dynamically adjust their frequency of operation [1], radiation pattern [2], and polarization [3] while maintaining a dense footprint. Reconfigurable antennas have regained a wide research interest as a low-cost solution to introduce modifiable features in multi-functional communication systems [4]. The fundamental feature of a reconfigurable antenna is the ability to modify its functional operating characteristics compared to a conventional antenna. Since traditional antenna characteristics (frequency, radiation pattern, and polarization) are fixed, multiple antenna elements are normally required in diverse applications such as multiple-input and multiple-output (MIMO), body-centric wireless communication (BWC) and cognitive radio [5].

The omnidirectional pattern generated by planar monopole antennas remains one of the desirable features of the antenna together with its reduced profile and ease in fabrication. However, the need to focus an antenna's beam in a specific direction does not only provide improved signal coverage and reduced power required in transmission but can also introduce nulls in the radiation pattern to avoid significant signal interference in multipath applications [6, 7]. As part of efforts, many pattern-reconfigurable antennas have been recently studied for both narrowband and wideband applications. In [8, 9, 10], switchable loaded-parasitic elements based on RF PIN diodes were investigated to achieve symmetrical patterns in specific operating modes. In these works, broadband radiation was achieved over a wideband by switching antenna elements at different angles to serve as reflectors in directing the main beam.

Another popular method proposed in [11, 12] involves the switching of the feed network that selects the appropriate excitation paths of the radiating elements. The complex antenna structure in [11] is designed to switch between a monopolar patch and an L-shaped fed circular patch in order to realize conical and broadside radiation patterns, respectively. Meanwhile, large microstrip patch antennas displaced at an angle of 45° were also shown to generate broadside reconfigurable patterns from +30° to -30° at 2.43 GHz in [2]. It is observed that the featured pattern-reconfigurable antennas lack a stable resonant frequency and compact sizes which discourages their use in space stringent applications. This instability in frequency is primarily due to the characteristic linkage property of antennas operating as circuits and resonators. One of the major goals in designing a reconfigurable antenna is to ensure the variation in one property has no effect on other properties of the antenna. To this end, the realization of a truly independent reconfigurable antenna whose characteristics are mutually exclusive of each other remains a major challenge [6].

Additionally, the polarization of the reconfigurable antenna plays a key role in its far-field characteristics. By this, the circular polarization of the antenna is necessary to maintain the communication link in

* Corresponding author.
E-mail address: smellis.coe@knust.edu.gh (M.S. Ellis).

https://doi.org/10.1016/j.heliyon.2022.e11721
Received 16 March 2022; Received in revised form 15 May 2022; Accepted 10 November 2022

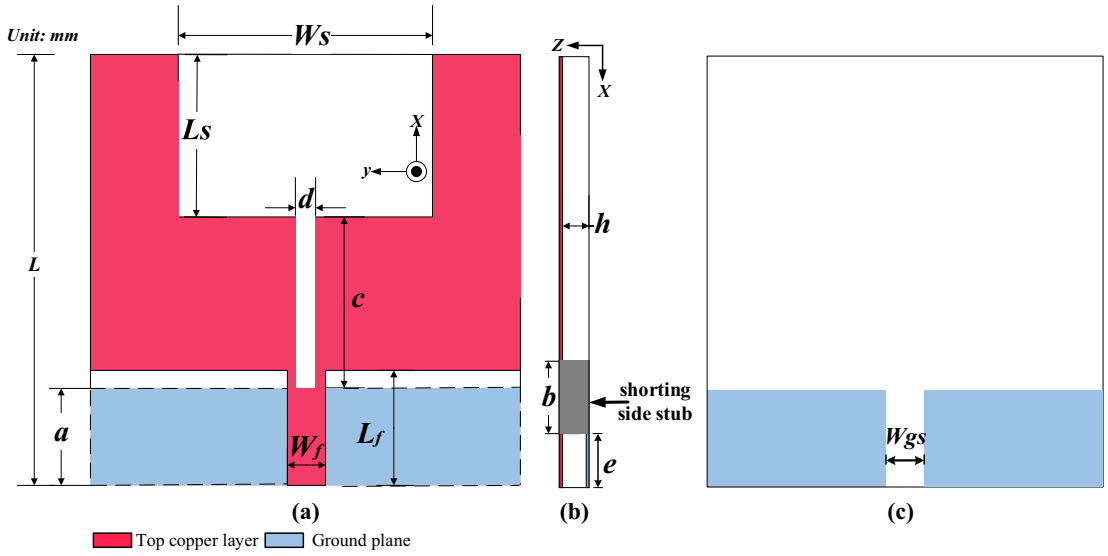

Figure 1. Design configuration of the flexible pattern-reconfigurable antenna. (a) top layout; (b) side layout; (c) back view.

Table 1. Optimized dimensions of the pattern-reconfigurable antenna.

Dimension	Value (mm)	Dimension	Value (mm)
L	28.8	a	4.44
L_s	10.37	b	1.50
L_f	5.43	c	14.0
W_s	15.28	d	0.62
W_f	1.26	e	4.0
h	0.25	W_{gs}	0.93

multipath applications. Some reconfigurable techniques have been recently studied to switch between left-hand circularly polarized (LHCP) and right-hand circularly polarized (RHCP) states in a linearly polarized (LP) aperture-coupled patch antenna [13]. In this work, embedded slots in the ground plane used in feeding the patches were sequentially excited in clockwise and anticlockwise directions using two PIN diodes to obtain equal but orthogonal currents of radiation. It was also demonstrated in [14] that, the switching of rectangular stubs along a coplanar waveguide (CPW) fed monopole antenna leads to an asymmetric structure that produces CP waves at the sub-6 GHz band. However, it is noted in these

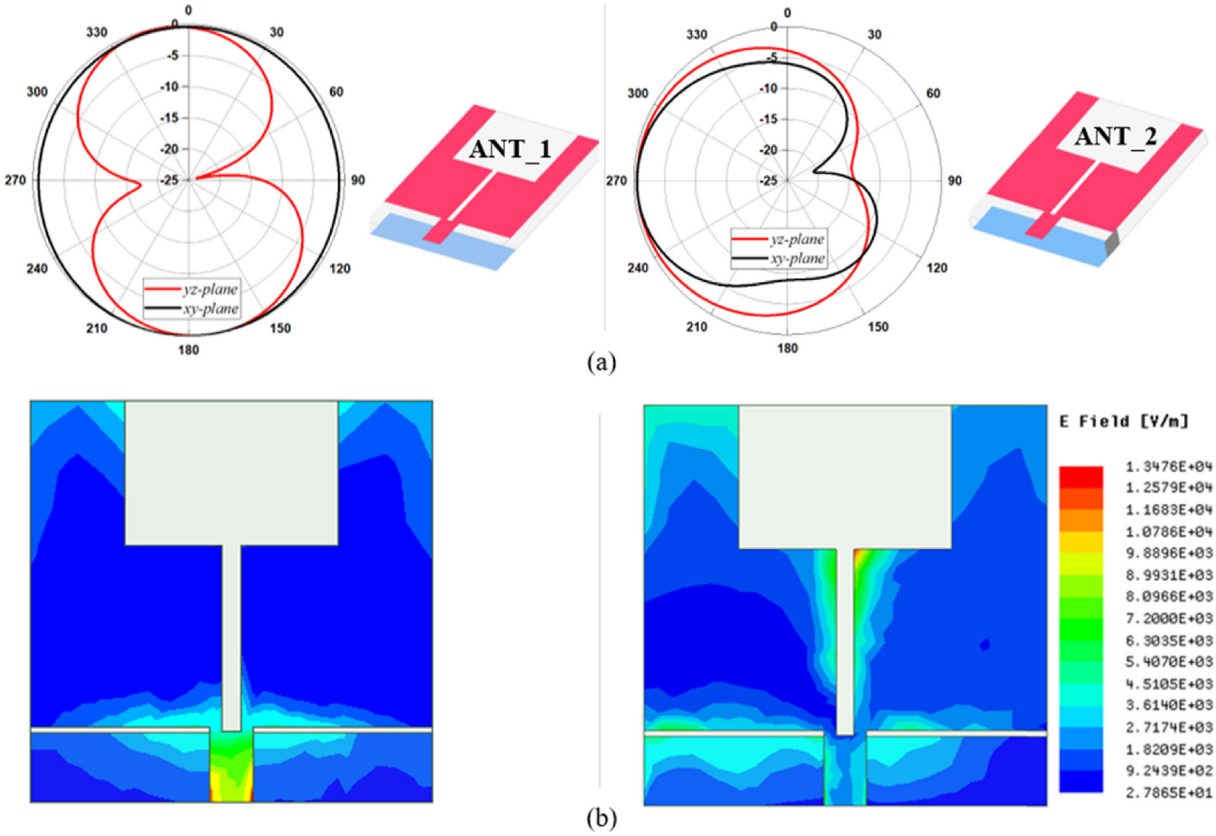

Figure 2. Combined simulated results of ANT_1 and ANT_2. (a)Radiation pattern (b) Surface current distribution at 2.45 GHz (ANT_1 – without side stub, ANT_2– with side stub).

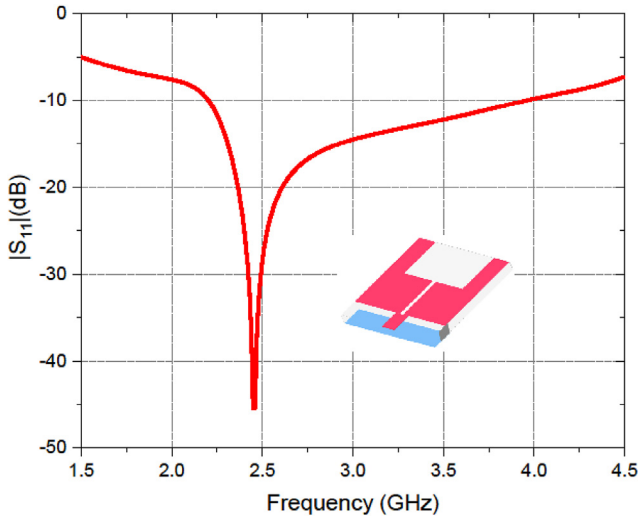

Figure 3. Simulated S_{11} of the single side-stub monopole antenna.

works that variation in the polarization states leads to slight detuning in the resonance due to the linkage effect discussed.

In this current work, a compact, circularly polarized pattern-reconfigurable antenna with conformable features based on an edge-stubbed radiator is demonstrated for applications in the 2.45 GHz ISM band. The design and implementation of the low-profile printed monopole antenna is presented in structured sections as follows. The single side-stub design for unidirectional radiation is reported in section two (2) while section three (3) introduces the pattern reconfiguration feature by incorporating RF PIN diodes. Further detailed implementation of the dual-stubbed reconfigurable antenna and the characteristics of linkage decoupling are also presented in section. A prototype of the fabricated antenna together with the simulated and measurement results are also discussed in section four. Meanwhile, conformability tests of the antenna under various bending scenarios and switching configurations are demonstrated followed by the main conclusions in the last section of the paper.

In general, the motivation for conducting this study is to provide a better and more-efficient radiator of electromagnetic energy in body-centric applications compared to the previous aforementioned works. Additionally, the addition of a reconfigurable application provides a flexible option of switching between desired radiation and reception points.

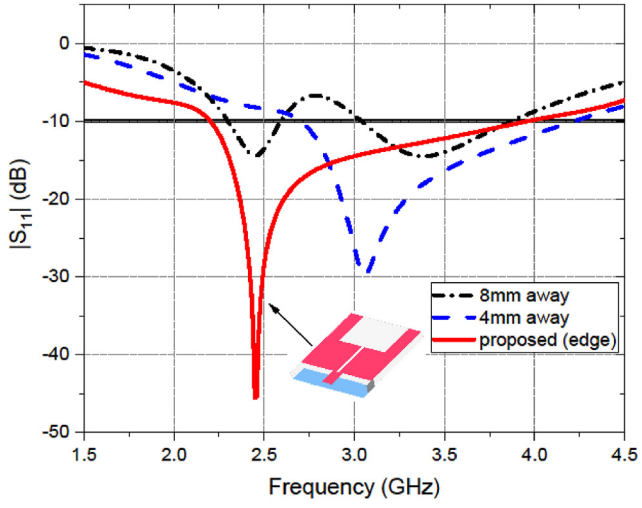

Figure 4. Effects of stub position along the $y-$ axis on reflection coefficient of the antenna.

2. Research methods

2.1. Antenna design and configuration

2.1.1. Single side-stub antenna design

Previous designs based on planar monopole antennas (PMAs) for body-centric applications possess omnidirectional patterns. Various techniques for realizing directional patterns in PMAs involve slotted-parabolic [15], defected, and full ground plane modifications. Here, the conventional omnidirectional pattern of the proposed antenna is converted into a directional pattern by using the novel quasi-radiator technique by *Ellis et.al* [16]. The front view, side stub, and ground plane of the pattern-reconfigurable antenna are shown in Figure 1(a) – (c).

Based on Figure 1, the design layout of the low-profile circularly polarized PMA consists microstrip fed, slotted-stepped rectangular radiators on a $h = 0.25$ *mm* thick FR-4 substrate. A partial ground plane with a rectangular slot is printed at the back of the antenna to improve impedance matching and bandwidth at the resonant frequency.

The overall topology measures a square compact size of $0.235\lambda_0$ ($\lambda_0 =$ free space wavelength at 2.45 GHz) with the optimized dimensions simulated in the HFSS software. Optimized dimensions of the antenna are shown in Table 1.

The shorted side-stub connects one arm of the slotted-stepped monopole to the rectangular ground plane which leads to the conduction of surface currents that are out-of-phase with the adjacent radiator arm and the ground plane. In this way, the shorted arm becomes non-radiative and acts as a reflector to steer the broadside radiation towards the $-y$ axis, similar to the operating principles in [16] and [17].

The radiation mechanism of the antenna can be understood by comparing the simulated antenna without a side stub in Figure 2(a) with the same antenna having an optimized side stub. It is observed from the surface current distribution that ANT_1 exhibits a regular omnidirectional radiation pattern as expected. However, a unidirectional pattern concentrated in the $-y$ direction is produced in both the azimuth and elevation planes when a simple stub is embedded at the right edge of the monopole in ANT_2. This is validated by the dominance of the surface current distribution on the left monopole as illustrated in Figure 2(b).

2.1.2. Determination of resonant frequency

The estimation of the lower resonant frequency of a regular-shaped planar monopole antenna is calculated from its physical dimensions corresponding to the equivalent area of a cylindrical monopole of the same length L and radius r [18], given by the relation as shown in Eq. (1):

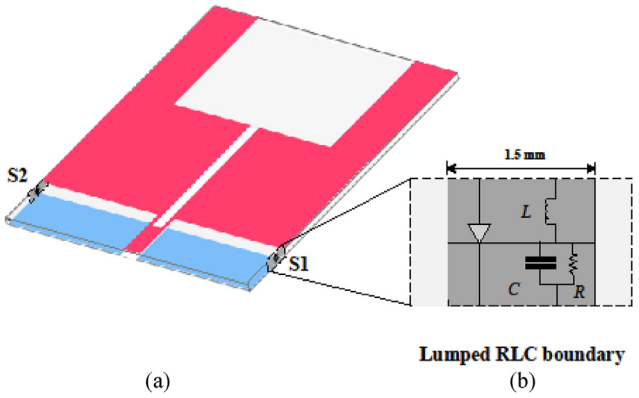

Figure 5. The pattern-reconfigurable monopole antenna. (a) Design of the dual-stubbed pattern-reconfigurable monopole antenna. (b) Equivalent PIN diode modelling of the side-stub as lumped *RLC* boundary.

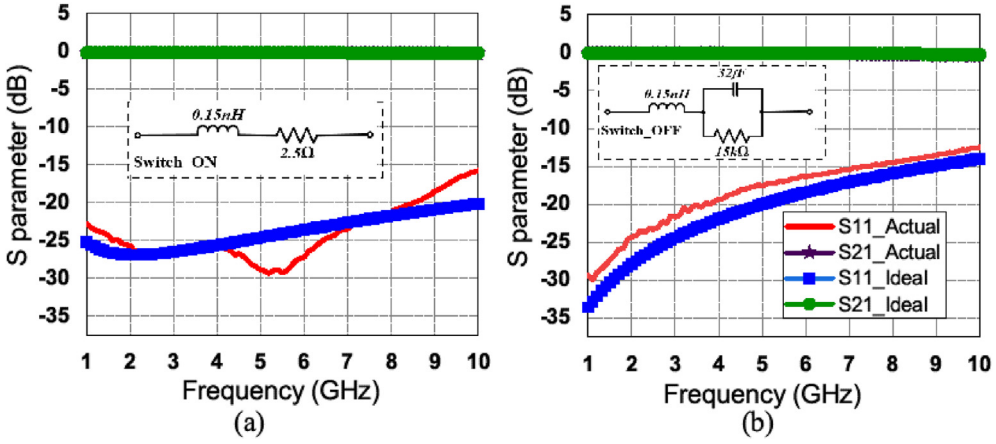

Figure 6. Equivalent PIN diode circuit model simulation. (a) Forward biased (b) Reverse biased.

$$2\pi rL = LW \tag{1}$$

For printed square monopole antennas (PSMA) of width, $W = L$, then the value of the radius is determined by Eq. (2).

$$r = \frac{L}{2\pi} \tag{2}$$

Hence, the lower resonant frequency F_l of the square monopole is determined by Eq. (3);

$$F_l = \frac{7.2}{(L + P + r)}\ [\text{GHz}] \tag{3}$$

Where L, r and the probe length p are in centimeters. From Eqs. (2) and (3), the PSMA with dimensions $L = 2.88\ cm$, and $p = 0.01\ cm$ yields $F_l = 2.15\ GHz$ for a reflection coefficient, $|S_{11}| \approx -10\ dB$. These initial parameters demonstrate resonance and is further optimized to achieve the desired resonance at 2.45 GHz as shown in Figure 3. The effect of the stub position along the y-axis on reflection coefficient of the antenna in shown in Figure 4.

2.1.3. *Effects of the shorting side stub*

As discussed earlier, the introduction of the side stub causes existing symmetric currents on the shorted radiator arm to be out-of-phase thereby acting as a reflector to generate broadside pattern in the opposite axis. From Figure 4, the optimal placement (i.e., edge) of the side stub is observed to achieve an improved $|S_{11}| < -20\ dB$ at 2.45 GHz. However, moving the stub 4 mm away from the edge in the $-y$ direction results in a shift in the resonance to about 3.05 GHz. Moving the stub 8 mm farther from the edge, the S_{11} deteriorates and the antenna loses its unidirectionality. Furthermore, the stub action introduces the necessary perturbation by producing equal magnitude but out-of-phase magnetic and electric currents on the shorted monopole arm.

In this way the degenerate modes are detuned at the targeted frequency. Hence, for the right edge-stubbed monopole antenna, a left hand

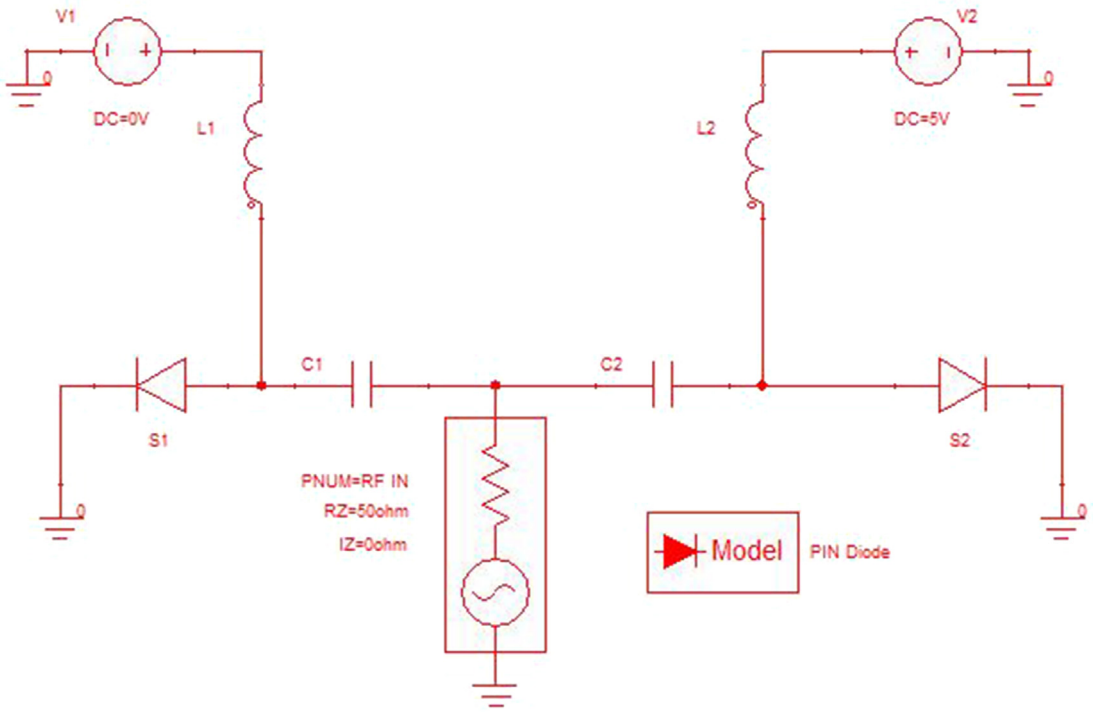

Figure 7. Schematic diagram of DC bias circuit of the proposed pattern-reconfigurable antenna.

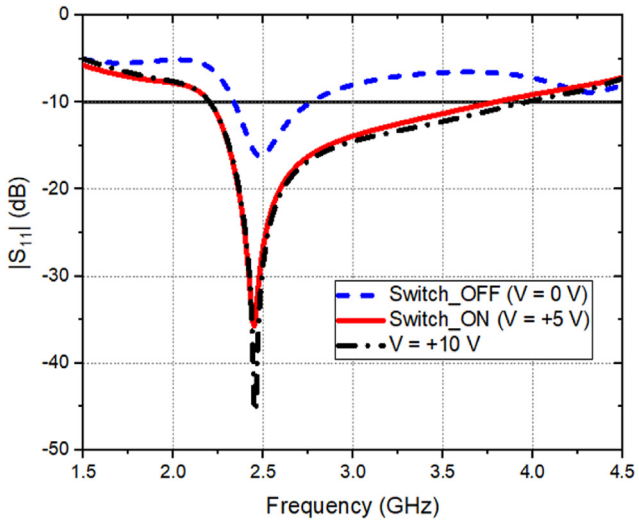

Figure 8. Simulated S_{11} of the proposed antenna under varying operating voltages.

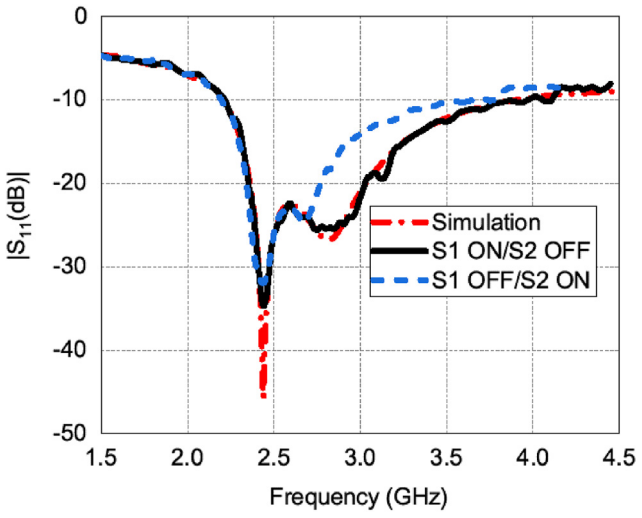

Figure 10. Simulation and Measured S_{11} of the fabricated antenna in Mode-1 and Mode-2.

Table 2. Operating modes and biasing configuration of the pattern-reconfigurable antenna.

Operating Mode	S1	S2	V1	V2
Mode-0	OFF	OFF	0V	0V
Mode-1	ON	OFF	+5V	0V
Mode-2	OFF	ON	0V	+5V

circularly polarized (LHCP) radiation can be formed. This is evident in the simulated axial ratio with a broadside radiation < 3 *dB* at the resonant frequency.

2.2. Pattern-reconfigurable antenna design

2.2.1. Design and principle of operation

Based on the single side stub design concept introduced in the previous section, it is observed that alternating the stub to connect either half of the monopole to the ground plane results in a symmetric broadside radiation pattern in the $\pm y$ directions. In this way, a reconfigurable extension of the antenna can be developed by incorporating RF PIN diodes to automate the switching of the radiation patterns. As a proof of concept, the RF switches S1 and S2 are modeled as an equivalent lumped resistor, inductor and capacitor (RLC) perfect electric conductor (PEC) boundary in the high-frequency structure simulator (HFSS) to replace the metallic side stubs. The pattern-reconfigurable monopole antenna is illustrated in Figure 5. Figure 5(a) shows the design with the attached switch and Figure 5(b) shows the lumped circuit of the attached switch.

Thus, when the switch is in the ON state (forward-biased), the equivalent circuit of the PIN diode is ideally represented as a series 2.5 Ω resistor and 0.15 *nH* inductor while the OFF state (reverse-biased) is modeled as a shunt combination of a 15 $k\Omega$ resistor and a 32 *fF* capacitor in series with the inductor [19] (zoom-in – Figure 5). Hence, the RLC boundary can be considered as the equivalent RF switch and their ON or OFF states basically represent the short or open circuit conditions of the side stubs respectively.

These ideal characteristics of the modeled PIN diodes exhibit a low return loss ($|S_{11}| < -20$ *dB*) in the ON condition with high isolation in the OFF state better than −15 dB within a wide band. However, implementation of the actual PIN diode presents real characteristics that are expected to differ from the ideal case due to several factors including parasitic losses. The DSM8100-000 beam-lead PIN diode with a very low total capacitance ($C_T = 0.025\,pF$) and small internal resistance in the range of $Rs = 2.5 - 3.5\,\Omega$ from Skyworks Inc [20]. is investigated for this work. The simulated return loss and isolation of the actual PIN diode are found to agree well with

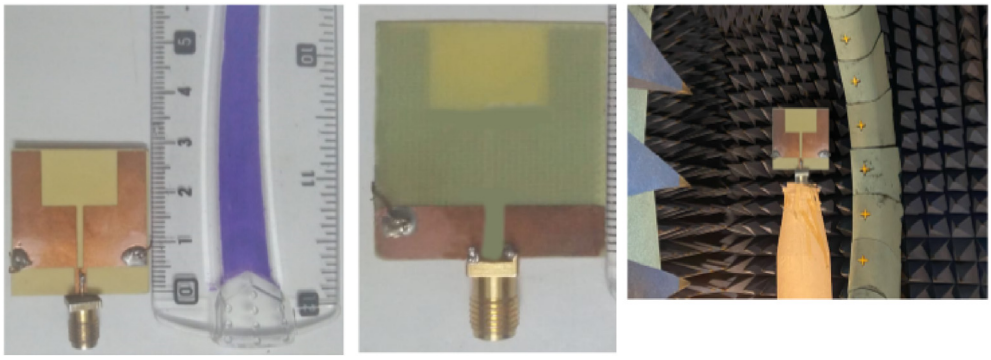

Figure 9. The fabricated prototype of the reconfigurable antenna. (a) front and a back view showing the realized PIN diode (b) far-field measurement in anechoic chamber.

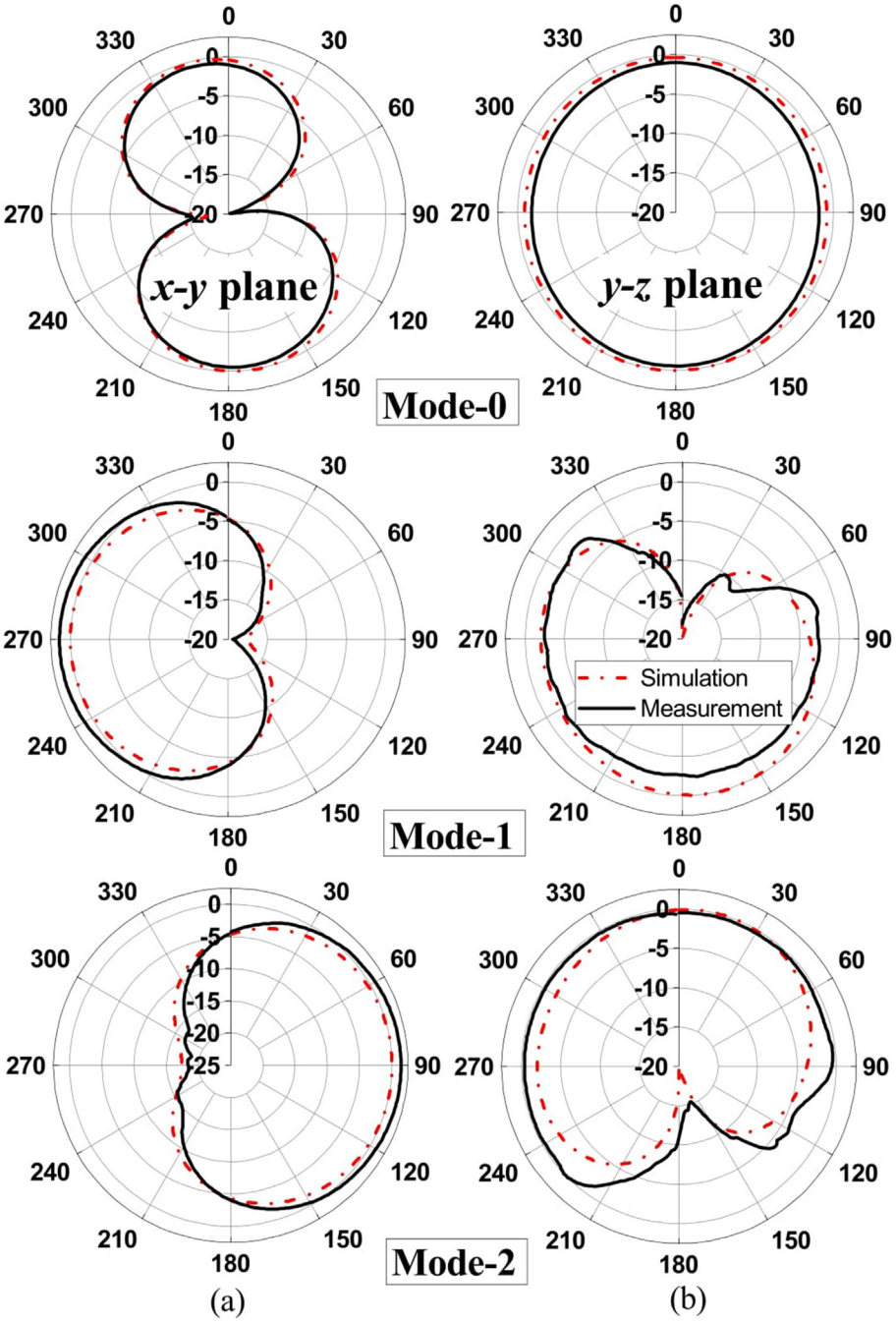

Figure 11. The normalized far-field patterns. (a) $x-y$ plane and (b) $y-z$ plane, between the simulated and measured results.

the ideal diode. An equivalent PIN diode circuit model simulation is shown in Figure 6. Figure 6 shows the S_{11} simulation of the proposed when switch is in on-mode in Figure 6(a) and off-mode in Figure 6(b). Both show good results in S_{11} with a slightly better matching in the on-state as expected.

2.2.2. DC biasing and tuning

The DC biasing network required to switch the two PIN diodes, S1 and S2 is designed to primarily isolate the RF and DC signal paths as shown in Figure 7.

The two PIN diodes are controlled by a simple shunt single pole double throw (SPDT) switch configuration which offers a high isolation with a very low insertion loss over a broad frequency range. The isolation (*Iso*) is found to be approximately 21 dB in the OFF state from the given Eq. (4) below [21],

$$I_{so} = 20 \log \left(1 + \frac{Z_0}{2R_s}\right) \tag{4}$$

Where *Rs* is the diode's series resistance at an input impedance characteristic $Z_0 = 50\ \Omega$.

From the design structure of the antenna, the left and right edges of the monopole are directly connected to the ground plane by the PIN diodes and therefore do not require additional capacitors to separate the DC and RF signals. Thus, only two blocking capacitors $C_1, C_2 = 1\ \mu F$ and two RF chokes $L_1, L_2 = 0.1\ \mu H$ are needed to prevent the RF currents from flowing back into the bias circuit before connecting them to the external DC bias voltages V_1 and V_2 respectively. Voltages V_1 and V_2 alternately biases the PIN diodes and are supplied at 0 V and 5 V to turn S1 and S2 ON and OFF respectively.

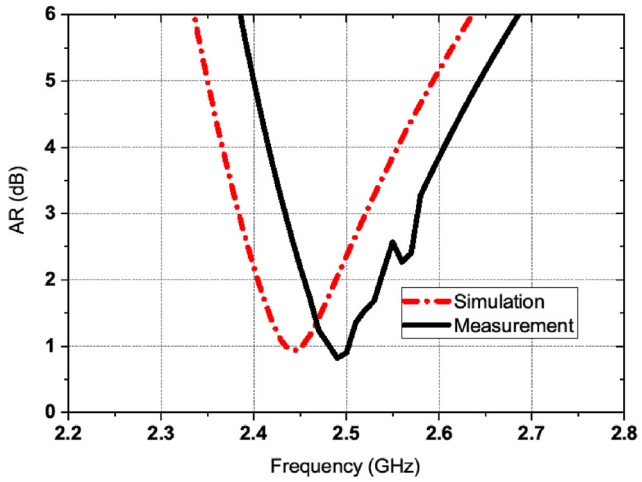

Figure 12. Simulated and Measured broadside axial ratio of the proposed antenna.

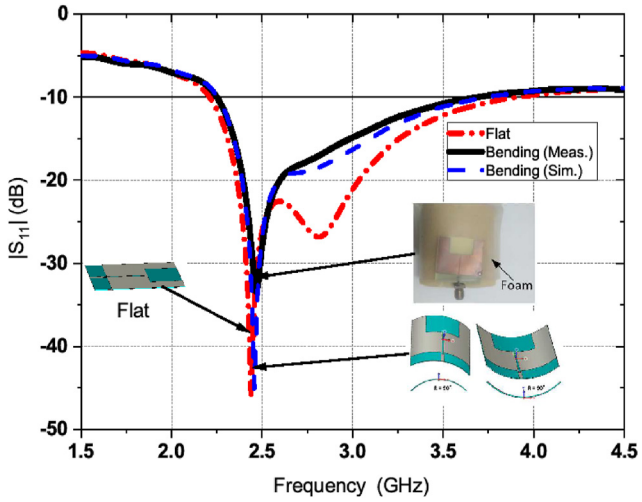

Figure 13. Simulated and Measured S_{11} of the proposed antenna in flat and bending configurations.

The reflection coefficient of the proposed reconfigurable antenna operating in different modes of supplied voltages is illustrated in Figure 8.

The bias voltages for Mode-1 and Mode-2 are varied between V_1 and V_2. V_1 is fixed at 0 V while V_2 is being varied and vice versa. It can be observed from the simulation that an increase in the supply voltage only improves the reflection coefficient of the antenna while the resonant frequency remains unaffected. This effect explains the decoupled frequency-radiation pattern characteristic linkage that most reconfigurable antennas suffer from [22, 23]. In this way, the switching of the antenna's radiation pattern does not have any effect on the operating frequency. Moreover, the input impedance of the antenna is well matched with a $VSWR < 2:1$. Altogether, the antenna can switch between three modes, i.e., the omnidirectional mode (Mode-0) and the two symmetrical modes of -90° (Mode$-$1) and $+90^\circ$ (Mode$-$2). The switching modes of S1 and S2 along with their respective voltage configurations are presented in Table 2.

2.3. Antenna fabrication and measurements

The FR4 substrate material is chosen for the fabrication of the reconfigurable antenna due to its low loss tangent ($\delta = 0.025$), low cost and easy availability. The front view, back view and view of the measurement setup in the anechoic chamber are shown in Figures 9(a), 9(b), and 9(c), respectively.

A simple soldering method is employed in the implementation of the RF PIN diodes. However, for best results and higher suppression of parasitics, the sophisticated thermocompression bonding technique which involves the pressing of the beam leads against the metalized antenna and the substrate under proper conditions of heat and pressure is recommended [19]. In this work, the standard 50 Ω SMA connector along with the coaxial cable is attached to the fabricated antenna and the $|S_{11}|$ is being measured using the PNA E8363C Agilent Network Analyzer. The simulated and measured$|S_{11}|$ less than 20 dB for Mode-1 and Mode-2 are shown in Figure 10. The far field radiation pattern measurements were also carried out in a pyramidal anechoic chamber (500 MHz–40 GHz) with Emerson and Cuming absorber. The normalized $x-y$ (E-) plane and $x-y$ (H-) plane far-field radiation patterns are illustrated in Figure 11(a) and Figure 11(b), respectively. In Mode-0, typical monopole-like radiation is observed while symmetric unidirectional patterns concentrated at -90° and $+90^\circ$ in the azimuth and elevation angles are exhibited for Mode-1 and Mode-2 respectively. Meanwhile, stable radiation patterns with no significant offsets are observed across the target bandwidth.

Moreover, the 3-dB AR bandwidth of the antenna is found to be 140 MHz (2.38 GHz $-$2.52 GHz). The simulated and measured broadside axial ratio of the proposed antenna is shown in Figure 12.

Additionally, to demonstrate conformability of the antenna and its potential for use in on-body applications, a flexible version of the FR-4 substrate is selected for further analysis.

Based on Figure 13, the reconfigurable antenna is subjected to bending at different degrees along the x and $y-$ axis and its corresponding S_{11} results are simulated and measured against the planar unbend configuration (flat). For conciseness, the bending angle $R = 90^\circ$ for inward and outward bending conditions is presented. The results show excellent agreement between the simulated and measurement with no significant variation in the reflection coefficient.

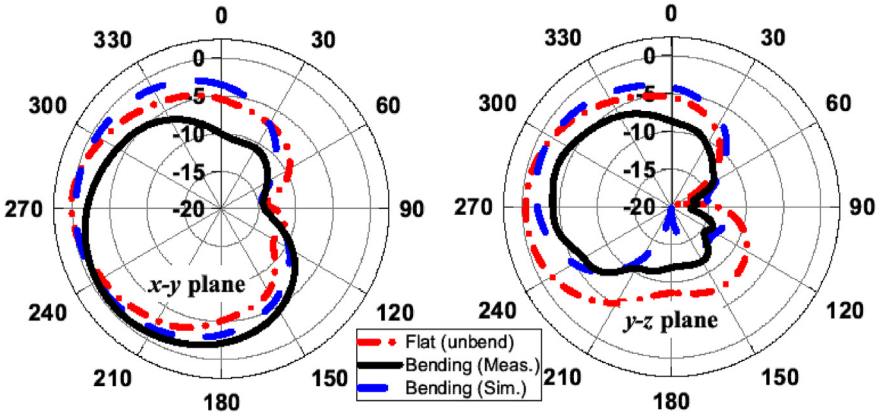

Figure 14. Simulated and Measured radiation pattern of the proposed antenna in flat (unbend) and bending configurations.

Table 3. Comparison of antenna characteristics and performance.

Reference	Overall Antenna size	$\lvert S_{11}\rvert < -10$ *dB* bandwidth (%)	Reconfigurable type	Frequency shift under tuning	Polarization/AR< 3 dB bandwidth
[8]	$0.16\ \lambda_0^2 \times 0.02\ \lambda_0$	66.67	Rad. Pattern (0°, ±90°)	N/A	Linear/ –
[9]	$0.02\ \lambda_0^2 \times 0.008\ \lambda_0$	2.02	Rad. Pattern (30°, 90°, 150 °)	1 GHz	Linear/ –
[11]	$1.64\ \lambda_0^2 \times 0.13\ \lambda_0$	23.5	Rad. Pattern (0 °, 90°)	~50 MHz	Linear/ –
[13]	$1.129\ \lambda_0^2 \times 0.02\ \lambda_0$	9.7	Polarization	N/A	Circular/5.7%
[24]	$0.20\ \lambda_0^2 \times 0.013\ \lambda_0$	20.2	Rad. Pattern (omni, broadside)	~10 MHz	Linear/ –
[25]	$0.06\ \lambda_0^2 \times 0.001\ \lambda_0$	41.35	Frequency, Rad. Pattern (180°)	125 MHz	Linear/ –
This Work	$0.05\ \lambda_0^2 \times 0.002\ \lambda_0$	58.06	Rad. Pattern (0°, ±90°)	~0 MHz	Circular/5.7%

Similarly, radiation patterns under the bending effect of the antenna were observed with minimal offsets as shown in Figure 14. This verifies that the bending conditions do not have any significant linked effect on the impedance characteristics of the antenna. It is emphasized that due to symmetry other modes of the antenna performance are not shown for brevity. Comparison of antenna characteristics and performance as shown in Table 3.

3. Conclusion

In this paper, a compact low-profile unidirectional monopole antenna based on a rectangular shorted side stub with flexible properties operating in the ISM band has been reported. To extend the degree of freedom in the radiation and maintain the communication link, a pattern-reconfigurable mode of the antenna was implemented based on the switching configuration of incorporated RF PIN diodes. Measurement results of the fabricated prototype agree strongly with the simulation. The radiation pattern of the antenna was shown to be fully reconfigured with three independent modes of operation. Additionally, the proposed antenna was shown to be immune to detuning effects resulting from likely body deformations. The proposed antenna also shows low SAR levels without the use of complex large cavity-backed structures, unlike other designs. Additionally, the antenna exhibits circular polarization altogether possessing a simple structure with a compact robust form factor that is highly efficient for on-body communications. Future works will focus on increasing the switching angles from 0° to 360° in steps of 10°. This will make the design smarter for array system applications.

Declarations

Author contribution statement

Philip Arthur; Mubarak Sani Ellis: Conceived and designed the experiments; Performed the experiments; Analyzed and interpreted the data; Wrote the paper.

Abdul-Rahman Ahmed; Jerry John Kponyo: Analyzed and interpreted the data; Contributed reagents, materials, analysis tools or data.

Funding statement

This research did not receive any specific grant from funding agencies in the public, commercial, or not-for-profit sectors.

Data availability statement

No data was used for the research described in the article.

Declaration of interest's statement

The authors declare no conflict of interest.

Additional information

No additional information is available for this paper.

References

[1] S. Sam, H. Kang, S. Lim, Frequency reconfigurable and miniaturized substrate integrated waveguide interdigital capacitor (SIW-IDC) antenna, IEEE Trans. Antenn. Propag. 62 (3) (2014) 1039–1045.
[2] M.S. Khan, A.D. Capobianco, S.M. Asif, A. Iftikhar, B.D. Braaten, R.M. Shubair, A pattern reconfigurable printed patch antenna, in: 2016 IEEE Antennas Propag. Soc. Int. Symp. APSURSI 2016 - Proc., 1, 2016, pp. 2149–2150.
[3] Y.J. Sung, T.U. Jang, Y.S. Kim, A reconfigurable microstrip antenna for switchable polarization, IEEE Microw. Wireless Compon. Lett. 14 (11) (2004) 534–536.
[4] N. Nguyen-Trong, L. Hall, F. Christophe, in: A Frequency- and Pattern-Reconfigurable Center-Shorted Microstrip Antenna, 15, IEEE, 2016, pp. 1955–1958.
[5] J. Constantine, Y. Tawk, S.E. Barbin, C.G. Christodoulou, Reconfigurable antennas: design and applications, Proc. IEEE 103 (3) (2015) 424–437.
[6] J.T. Bernhard, in: Reconfigurable antennas, 4, 2007.
[7] H.C. Mohanta, A.Z. Kouzani, S.K. Mandal, Reconfigurable antennas and their applications, Univers. J. Electr. Electron. Eng. 6 (4) (2019) 239–258.
[8] T. Aboufoul, C. Parini, X. Chen, A. Alomainy, Pattern-reconfigurable planar circular ultra-wideband monopole antenna, IEEE Trans. Antenn. Propag. 61 (10) (2013) 4973–4980.
[9] C.M. Lee, C.W. Jung, Radiation-pattern-reconfigurable antenna using monopole-loop for Fitbit flex wristband, IEEE Antenn. Wireless Propag. Lett. 14 (2015) 269–272.
[10] Y.Y. Bai, S. Xiao, M.C. Tang, C. Liu, B.Z. Wang, Pattern reconfigurable antenna with wide angle coverage, Electron. Lett. 47 (21) (2011) 1163–1164.
[11] W. Lin, H. Wong, R.W. Ziolkowski, Wideband pattern-reconfigurable antenna with switchable broadside and conical beams, IEEE Antenn. Wireless Propag. Lett. 16 (2017) 2638–2641.
[12] A. Mahabub, M.N. Islam, M.M. Rahman, An advanced design of pattern reconfigurable antenna for Wi-Fi and WiMAX base station, in: 4th Int. Conf. Adv. Electr. Eng. ICAEE 2017, 2017, pp. 74–79.
[13] H. Gu, L. Ge, J. Zhang, Reconfigurable circular-ring feed patch antenna with tri-polarization diversity, Front. Physiol. 9 (2021), 752505.
[14] A. Ghaffar, X.J. Li, T. Ahmad, N. Hussain, M. Alibakhshikenari, E. Limiti, Circularly polarized pattern reconfigurable flexible antenna for 5G-sub-6-GHz applications, in: 2020 IEEE Asia-Pacific Microwave Conference (APMC), 2020, pp. 625–627.
[15] J. Golezani, M. Abbak, I. Akduman, Modified directional wideband printed monopole antenna for use in radar and microwave imaging applications, Progress in Electromagnetics Research Letters 33 (2012) 119–129.
[16] M.S. Ellis, A.-R. Ahmed, J.J. Kponyo, J. Nourinia, C. Ghobadi, B. Mohammadi, Unidirectional planar monopole antenna using a quasi-radiator, IEEE Antenn. Wireless Propag. Lett. 18 (1) (2019) 157–161.
[17] G.-M. Zhang, J.-S. Hong, B.-Z. Wang, G. Song, P. Zhang, Compact wideband unidirectional antenna with a reflector connected to the ground using a stub, IEEE Antenn. Wireless Propag. Lett. 10 (2011) 1186–1189.
[18] G. Li, M. Li, in: Broadband Microstrip Antennas, 26, 1998.
[19] M. Shirazi, J. Huang, T. Li, X. Gong, A switchable-frequency slot-ring antenna element for designing a reconfigurable array, IEEE Antenn. Wireless Propag. Lett. 17 (2) (2018) 229–233.
[20] Skyworks, DSM8100-000: Mesa Beam-Lead PIN Diode Applications, Data Sheet, 2008, pp. 1–5.
[21] W. Dorothy, R. Joos, in: The Pin Diode Circuit Designers' Handbook," Watertown, 617, 1998.
[22] J. Buckley, K.G. McCarthy, B. O'Flynn, C. O'Mathuna, The detuning effects of a wrist-worn antenna and design of a custom antenna measurement system," European Microwave Week 2010, EuMW2010: connecting the World, Conference Proceedings - European Microwave Conference, EuMC (2010) 1738–1741, 2010, no. September.
[23] S.P. Pinapati, S.J. Chen, D. Ranasinghe, C. Fumeaux, Detuning effects of wearable patch antennas, in: Asia-Pacific Microwave Conference Proceedings, APMC, 2017, pp. 162–165.
[24] Zakaria Mahlaoui, Eva Antonino-Daviu, Miguel Ferrando-Bataller, Radiation pattern reconfigurable antenna for IoT devices, Int. J. Antenn. Propag. (2021) 2021. Article ID 5534063, 13 pages.
[25] A. Ghaffar, X.J. Li, W.A. Awan, A.H. Naqvi, N. Hussain, M. Alibakhshikenari, E. Limiti, in: A Flexible and Pattern Reconfigurable Antenna with Small Dimensions and Simple Layout for Wireless Communication Systems Operating over 1.65–2.51 GHz, 10, Electronics, Switzerland, 2021, pp. 1–13.